The *C. elegans* homologs of nephrocystin-1 and nephrocystin-4 are cilia transition zone proteins involved in chemosensory perception

Marlene E. Winkelbauer[1], Jenny C. Schafer[1], Courtney J. Haycraft[1], Peter Swoboda[2] and Bradley K. Yoder[1,*]

[1]Department of Cell Biology, University of Alabama at Birmingham Medical Center, Birmingham Alabama, 35294, USA
[2]Karolinska Institute, Department of Biosciences, Södertörn University College, Section of Natural Sciences, S-14189 Huddinge, Sweden
*Author for correspondence (e-mail: Byoder@uab.edu)

Accepted 23 August 2005
Journal of Cell Science 118, 5575-5587 Published by The Company of Biologists 2005
doi:10.1242/jcs.02665

Summary

Nephronophthisis (NPH) is a cystic kidney disorder that causes end-stage renal failure in children. Five nephrocystin (nephrocystin-1 to nephrocystin-5) genes, whose function is disrupted in NPH patients, have been identified and data indicate they form a complex at cell junctions and focal adhesions. More recently, the nephrocystin proteins have also been identified in cilia, as have multiple other cystic kidney disease related proteins. Significant insights into this cilia and cystic kidney disease connection have come from analyses in simpler eukaryotic organisms such as *Caenorhabditis elegans*. In this regard, we became interested in the *C. elegans* homologs of nephrocystin-1 (*nph-1*) and nephrocystin-4 (*nph-4*) from a database screen to identify genes coordinately regulated by the ciliogenic transcription factor DAF-19. Here we show that expression of *nph-1* and *nph-4* is DAF-19 dependent, that their expression is restricted to ciliated sensory neurons, and that both NPH-1 and NPH-4 concentrate at the transition zones at the base of the cilia, but are not found in the cilium axoneme. In addition, NPH-4 is required for the localization of NPH-1 to this domain. Interestingly, *nph-1* or *nph-4* mutants have no obvious cilia assembly defects; however, they do have abnormalities in cilia-mediated sensory functions as evidenced by abnormal chemotaxis and lifespan regulation. Our data suggest that rather than having a ciliogenic role, the NPH proteins play an important function as part of the sensory or signaling machinery of this organelle. These findings suggest that the defects in human NPH patients may not be the result of aberrant ciliogenesis but abnormal cilia-sensory functions.

Supplementary material available online at
http://jcs.biologists.org/cgi/content/full/118/23/5575/DC1

Key words: Cilia, Transition zone, Chemosensation, X-box, Cystic kidney disease

Introduction

Nephronophthisis (NPH) is a group of autosomal recessive cystic kidney disorders resulting in chronic renal failure in children. NPH patients share features of renal cyst development at the corticomedullary junction along with irregularities in tubular basement membrane, tubular atrophy, interstitial cell infiltration, and renal fibrosis (Hildebrandt and Omram, 2001; Hildebrandt and Otto, 2000). Mutations in five genes (nephrocystin-1 to 5) have been identified in patients with nephronophthisis (Olbrich et al., 2003; Otto et al., 2002; Otto et al., 2000; Otto et al., 2003; Otto et al., 2005); however, the function of these proteins and the mechanism by which their disruption leads to the renal pathology remains fundamentally unknown.

The best characterized of the nephrocystin proteins is nephrocystin-1 (Otto et al., 2000). Nephrocystin-1 has several protein interaction modules including N-terminal coiled-coils, a Src homology 3 (SH3) region, and a nephrocystin homology domain (NHD) located in the C-terminal 2/3 of the protein. Data in mammalian systems suggest that nephrocystin-1 functions as a docking protein involved in cytoskeletal organization and cell adhesion regulation at focal adhesions and at cell-to-cell junctions. This is based on binding studies showing that mammalian nephrocystin-1 interacts with adaptor proteins such as proline-rich tyrosine kinase 2, p130cas, and actin binding proteins tensin and the filamins (Benzing et al., 2001; Donaldson et al., 2000; Donaldson et al., 2002). Recently, it was demonstrated that mammalian nephrocystin-1 associates with nephrocystin-4 (Mollet et al., 2005). In addition, nephrocystin-2 and nephrocystin-3 are co-immunoprecipitated with nephrocystin-1 antibodies (Olbrich et al., 2003; Otto et al., 2003), thus, leading to the speculation that these four nephrocystin proteins form a complex and function in the same pathway.

In addition to the localization of nephrocystin-1 to sites of cell contact and the focal adhesions, mammalian nephrocystin-1 and nephrocystin-4 have been detected in primary cilia and basal bodies at the base of cilia. They are thought to bind to β-tubulin, the central component of the cilium axoneme in mammalian cells (Mollet et al., 2005; Otto et al., 2003). In addition, the nephrocystin-4 homolog in *Chlamydomonas* has been shown to be a component of the centriole and the basal body (Keller et al., 2005). Localization to cilia has also been reported for nephrocystin-2 (also known as inversin) and

nephrocystin-5 (Otto et al., 2003; Otto et al., 2005). Whereas nephrocystin-3 has not yet been identified in cilia, the interaction of nephrocystin-3 with the other nephrocystins makes this probable (Olbrich et al., 2003). Thus, the current theory is that the nephrocystins form a multifunctional complex that mediates signaling activity in actin and microtubule based structures; however, the role that this complex plays in these regions of the cell remains unknown.

Cilia are microtubule based organelles that extend from most cells in the mammalian body. They are assembled through an evolutionarily conserved process called intraflagellar transport (IFT) that mediates the anterograde and retrograde movement of protein complexes along the axoneme (Kozminski et al., 1993; Scholey, 2003). Disruption of IFT in mice results in loss of cilia and leads to severe developmental and disease pathologies (Murcia et al., 2000; Pazour et al., 2000; Zhang et al., 2004). Intriguingly, many human and murine disorders whose pathology is characterized by renal cyst formation have now been associated with cilial proteins (Pazour, 2004; Zhang et al., 2004) thus highlighting the importance of this organelle in normal renal physiology.

Our understanding of the function of several of the cystic kidney disease-related proteins that localize in the cilia has benefited greatly from the analysis of their homologs in simpler eukaryotic organisms such as *Chlamydomonas* and *C. elegans*. For example, the homologs of the cystic kidney disease genes *Tg737* (*osm-5*) (Haycraft et al., 2001), polycystin-1 (*lov-1*) and polycystin-2 (*pkd-2*) (Barr et al., 2001) have been characterized in *C. elegans* and all three of these proteins have been detected in the cilia of sensory neurons. Loss of *lov-1* or *pkd-2* function has no overt effects on the assembly or morphology of the cilia; however, it does impair cilia-mediated signaling events required for the male to locate the hermaphrodite vulva, resulting in abnormal male mating behavior. In contrast to *lov-1* and *pkd-2*, disruption of *osm-5* results in defects in cilia assembly. Characterization of the OSM-5 protein revealed that it is a key component of the IFT particle (Haycraft et al., 2001; Qin et al., 2001). The OSM-5 protein concentrates at the transition zone at the base of the cilium and in a punctate pattern along the cilium axoneme typical of other IFT proteins. As seen with *C. elegans* lacking *lov-1* or *pkd-2*, *osm-5* mutants exhibit male behavioral defects, as do other IFT mutants in *C. elegans*. Thus, the mating defect is probably caused by the loss of cilia on sensory neurons of the male that are required for *lov-1* and *pkd-2* signaling function. In addition to mating abnormalities, *osm-5* and other IFT mutants have defects in chemotaxis, dauer formation, dye-filling, osmotic avoidance, and have extended lifespan, all of which are thought to be caused by loss of cilia and consequently cilia-mediated sensory activity on these neurons (Apfeld and Kenyon, 1999; Starich et al., 1995).

In order to understand the connection between cilia and cystic kidney disease, it is crucial that we identify and characterize additional cystogenic proteins involved in formation and function of cilia. In this regard, we previously described a database genome screen of *C. elegans* and *C. briggsae* to identify components of cilia (Haycraft et al., 2003; Schafer et al., 2003). This search was based on coordinate regulation of many ciliogenic genes by the DAF-19 transcription factor (Efimenko et al., 2005; Swoboda et al., 2000). DAF-19 regulation is mediated through a motif called an X-box that in *C. elegans* is normally located within the first few hundred bases upstream of the start of translation. Among the candidate genes obtained from our search for an X-box in putative promoter regions were many of the previously characterized IFT proteins, and intriguingly the *C. elegans* homologs of nephrocystin-1 (*nph-1*) and nephrocystin-4 (*nph-4*).

We describe two *C. elegans nph* genes and the NPH proteins and explore their possible function in ciliated sensory neurons. Our results indicate that both *nph-1* and *nph-4* are expressed in ciliated sensory neurons of the male and hermaphrodite in a DAF-19-dependent manner. We show that both NPH-1 and NPH-4 localize to the transition zones at the base of the cilia but not in the cilium axoneme and that NPH-4 is required for correct localization of NPH-1 to this domain. Intriguingly, disruption of either *nph* gene does not affect cilium formation but does result in impaired chemotaxis to volatile attractants and an extended lifespan. These findings along with previous results demonstrating male mating defects in *nph-1;nph-4* double mutants and in animals where *nph-1* or *nph-4* expression was reduced by RNAi suggest a role for the NPH-1 and NPH-4 proteins as part of the general sensory machinery at the transition zone at the base of cilia that is required for cilia-mediated signaling in response to changes in environmental stimuli (Wolf et al., 2005; Jauregui and Barr, 2005).

Materials and Methods

General molecular biology methods

Standard molecular biology procedures were conducted according to Sambrook et al. (Sambrook et al., 1989). *C. elegans* genomic DNA, *C. elegans* cDNA, single worms and cloned worm DNA were utilized for PCR amplifications, direct sequencing and subcloning as described previously (Sambrook et al., 1989). PCR conditions and reagents are available on request. DNA sequencing was performed by the UAB Genomics Core Facility of the Heflin Center for Human Genetics.

DNA sequence analyses

Genome sequence information was obtained from the National Center for Biotechnology Information (http://www.ncbi.nlm.nih.gov/) or from the Celera Database (http://www.celera.com), Gene sequences were identified using the *C. elegans* database Wormbase and references therein (http://www.wormbase.org). Sequence alignments and conserved motifs were identified using ClustalW (http://www.ebi.ac.uk/clustalw/) and the PileUp, and MotifSearch (MEME) algorithms associated with Wisconsin GCG program (Accelrys, Inc., http://www.accelrys.com/products/gcg_wisconsin_package/program).

A search of the *C. elegans* and the *C. briggsae* genomes was conducted utilizing a computer algorithm to identify potential target genes of the transcription factor DAF-19 as described previously (Haycraft et al., 2003; Schafer et al., 2003; Swoboda et al., 2000; Efimenko et al., 2005). This search involved the analysis of regions upstream of the ATG of predicted genes for the X-box promoter consensus sequence. The search identified a number of previously characterized IFT genes as well as *R13H4.1(nph-4)* in addition to the *C. briggsae* homolog of *M28.7(nph-1)*. Visual inspection of the *C. elegans nph-1* promoter revealed the presence of an X-box sequence that was not identified by the computer based search because of the presence of an extra nucleotide not included in the search algorithm. BLAST and visual inspection were used to identify and compare X-

box sequences found in the promoter regions of *C. briggsae* and mouse homologs of *nph-1* and *nph-4*.

Strains

Worm strains were obtained from the *Caenorhabditis* Genetics Center, *C. elegans* Knock-Out Consortium, and the National BioResource Project in Japan. The strains were grown using standard *C. elegans* growth methods (Brenner, 1974) at 20°C unless otherwise stated. The wild-type stain was N2 Bristol. The following strains were also used: RB743 *nph-1(ok500)II*, CB3970 *unc-4(e120)II*; *bli-1(e769)II*, JT6924 *daf-19(m86)II*; *daf-12(sa204)X*, JT204 *daf-12(sa204)X*, DR550 *osm-5(m184)X*, FX925 *nph-4(tm925)V* and YH278 *nph-1(ok500)II*; *nph-4(tm925)V*. YH192 yhEx119 (*tx: nph-1::CFP*) in N2, YH269 yhEx168 (*tx: nph-4::DsRed2*) in N2, YH238 yhEx150 (*tx: nph-1::CFP*;*tx: che-13::DsRed2*) in JT6924 and YH240 yhEx150 (*tx: nph-1::CFP*;*tx: che-13::DsRed2*) in JT204 were utilized for *nph-1* and *nph-4* expression analyses. YH220 yhEx138 (*tl: nph-1::CFP*;*tl: nph-4::YFP*), YH224 yhEx142 (*tl: nph-4::YFP*;*tl: che-13::CFP*) in N2, YH237 yhEx149 (*tl: nph-1::CFP*;*tl: che-13::YFP*) in N2, YH230 yhEx145 (*tl: nph-4::YFP*) in RB743, YH309 yhEx149 (*tl: nph-1::CFP;tl: che-13 YFP*) in FX925 were utilized for NPH-1 and NPH-4 protein localization analyses. YH307 yhEx185 (*tl: che-13::YFP*) in YH278 was utilized to measure cilia length in the double *nph* mutant background. YH317 yhEX193 (tl: *nph-1::GFP*) in RB743 and YH331 yhEx202 (tl: *nph-4::YFP*) in FX925 were utilized for rescue experiments. These rescue lines were generated using UNC-122::GFP (Loria et al., 2004) as a marker instead of *rol-6(su1006)* to examine chemotaxis rescue.

The RB743 strain was outcrossed three times using the closely linked CB3970 strain. The mutation in the resulting strain was confirmed by PCR. The YH278 double mutant strain was generated by crossing RB743 male worms with FX925 hermaphrodites. The resulting F2 offspring obtained from self fertilization were screened by PCR to identify strains containing both mutations.

Generation of constructs and strains

The vectors used for generating the promoter and genomic fusion constructs were modified from pPD95.81 (a gift from A. Fire). The pCJF6 vector was created by removing the GFP from pPD95.81 and replacing it with the CFP from pPD134.96 (Haycraft et al., 2003). Similarly, the pCJF7 vector was created by removing GFP from pPD95.81 and replacing it with YFP from pPD132.102. The pCJ102 vector was created by replacing the GFP from pPD95.81 with dsRed2 from pDsRed2 (Clontech, Palo Alto, CA, USA). The transcriptional *nph-1::CFP* vector (pCJ114) and the translational NPH-1::CFP vector (pCJ148) were created by inserting a 2 kb and a 3.6 kb fragment, respectively, into the pCJF6 vector, each containing 300 bp of the *nph-1* promoter amplified from N2 genomic DNA. A fragment containing 1 kb of the promoter of *nph-4* was generated by PCR from N2 genomic DNA and was cloned into vector pCJ102 to generate the transcriptional *nph-4::DsRed2* vector (pCJ162). In addition the promoter and the entire *nph-4* gene were cloned into vector pCJF7 to generate the translational NPH-4::YFP fusion construct pCJ146. Owing to the presence of two predicted genes contained in two introns of *nph-4*, the 5′ end of *nph-4*, including the predicted promoter, was amplified from N2 genomic DNA and the 3′ end of *nph-4* was amplified from *C. elegans* cDNA. These two fragments were ligated together at the *Cla*I site located at bp 1729 in the cDNA sequence and subsequently were cloned into pCJF7. Additional expression constructs used were the pCJ49.2 transcriptional *che-13::DsRed2*, which was previously described (Haycraft et al., 2003), pCJ36.1 translational CHE-13::CFP, and pCJ37.3 translational CHE-13::YFP. The transgenic strains above were generated as described previously (Mello et al., 1991). All PCR was performed using AccuTaq-LA DNA Polymerase (Sigma, St Louis, MO, USA) according to manufacturer's instructions.

Imaging

Worms were anesthetized using 10 mM Levamisole and were immobilized on a 2% agar pad for imaging. Worms were examined using a Nikon Eclipse TE200 inverted microscope and images captured with a CoolSnap HQ camera (Photometrics, Tucson, AZ, USA). Shutters and filters were computer driven. Images were processed using Metamorph software (Universal Imaging, Downingtown, PA, USA). Confocal analysis was performed on a Leica DMIRBE inverted epifluorescence/Nomarski microscope fitted with Leica TCS NT laser confocal optics and software (Leica. Inc.; Exton, PA, USA). Optical sections through the Z axis were generated using a stage galvonometer or step motor. Further processing of images was done using Photoshop 7.0 (Adobe Systems, Inc., San Jose CA, USA).

DAF-19 regulation

RNA was isolated as described previously (Haycraft et al., 2003) from JT204 and JT6924 mutants. Reverse transcribed RNA(cDNA) was generated using Superscript II Reverse Transcriptase (Invitrogen, Carlsbad, CA, USA) as per the manufacturer's instructions. PCR was performed using primers that result in amplification of fragments of 250 bp *(nph-1)*, 300 bp *(nph-4)* and 750 bp *(snt-1)*. *snt-1* served as an internal non-DAF-19 regulated control.

To test DAF-19 regulation in vivo, the transgenic line YH238 was generated by injection of *tx: nph-1::CFP* and *tx: che-13::DsRed2* into the JT6924 *daf-19(m86); daf-12(sa204)* mutant background. The YH238 strain was then crossed to the JT204 *daf-12(sa204)* strain resulting in the same extrachromosomal array being present in the *daf-19*(+) background. The strains used contain a mutation in *daf-12(sa204)X* to suppress the Daf-c phenotype of *daf-19(m86)II*.

The X-box sequence of the *nph-4* gene was mutated in the pCJ162 construct by performing site-directed mutagenesis, mutating the first three, the middle two and the last three bases, generating construct p255. This resulted in the X-box sequence, TAATCC TC GACTTG, mutated from the original X-box sequence, ATTTCC AT GACAAC. This construct, consisting of *tx: nph-4(Mut X-box)::DsRed2*, was co-injected into N2 worms along with *tx: osm-5::CFP*, which contains a functional X-box. Expression was examined in 18 individual F1 Rol offspring.

Assays

Dye-filling using DiI (Molecular Probes, Carlsbad, CA, USA) and osmotic avoidance assays were performed as described previously (Starich et al., 1995).

The ability of *C. elegans* strains to form dauer stages was tested as described previously (Starich et al., 1995). Briefly, mutant and wild-type 'starved' worms were collected and resuspended in 1 ml of 1% SDS solution. The worms were incubated with rocking for 1 hour and washed three times in sterile distilled water. Surviving worms were examined immediately after plating on bacterially seeded plates.

The lifespan assay used was adapted from Dorman et al. (Dorman et al., 1995; Gandhi et al., 1980). Worms were bleached to synchronize the population and the resulting eggs were seeded to fresh NGM plates and incubated at 20°C. The day the eggs were seeded was considered the day of hatching d=0. Upon reaching the L4 stage, the animals were picked to new plates containing 5-fluoro-2′-deoxyuridine (FUDR) (Sigma-Aldrich, St Louis, MO, USA) to inhibit growth of progeny. The animals were observed daily for survival, and dead worms were removed.

Chemotaxis assays to volatile attractants were performed essentially as described previously (Blacque et al., 2004). Briefly, 10 cm chemotaxis plates were made as described previously (Matsuura et al., 2004). A spot was marked at the center of each plate as well as at opposite sides, 0.5 cm from the edge. A zone was drawn at each side 1.5 cm from each of these spots representing the chemoattractant

zone and the control zone. To the spots in each zone 1 μl of 1 M sodium azide was added as an anesthetic. In the chemoattractant zone, 1 μl of chemoattractant (diluted 1:100 in 95% ethanol) was added and at the opposite control zone 1 μl of 95% ethanol alone was added. Young adult worms (50-150) were deposited in the center of the plate and were counted at 15-minute intervals over the course of 90 minutes. The efficiency of chemotaxis at each time point was calculated as the chemotaxis index: the number of worms at the chemoattractant zone minus the number of worms at the control zone divided by the total number of worms on the plate.

RT-PCR of *nph* gene expression in *nph-1(ok500)* and *nph-4(tm925)*

RNA was isolated as described previously (Haycraft et al., 2003) from *nph-1(ok500)* and *nph-4(tm925)* mutants. Reverse transcribed RNA was generated using Superscript II Reverse Transcriptase (Invitrogen, Carlsbad, CA, USA) as per the manufacturer's instructions. PCR was performed using primers that result in amplification of fragments crossing over the deleted region for each respective mutation and these fragments were sequenced. The results from the RT-PCR analyses of expression from the *nph-1* or *nph-4* mutant loci are included in the supplementary material Fig. S2.

Results

nph-1 and *nph-4* are expressed in ciliated sensory neurons

Previously, we described a genome sequence-based search to identify genes involved in ciliogenesis and cilia function in *C. elegans* (Haycraft et al., 2003; Schafer et al., 2003; Swoboda et al., 2000; Efimenko et al., 2005). Among the candidate genes obtained from this search were several homologs of mammalian genes known to be associated with cystic kidney disorders such as Bardet-Biedl Syndrome (BBS) (Blacque et al., 2004) and *nph-4* that is responsible for the renal pathology in juvenile nephronophthisis patients. The X-box motif in *nph-4* is located at position –168 relative to the translational start site and is near a consensus sequence with functional X-boxes identified in other genes (Table 1).

In addition to searching the *C. elegans* genome for X-box sequences this search was also conducted in the closely related worm *C. briggsae*. The promoter region of the *C. briggsae* homolog of the *nph-1* gene also contains a strong X-box sequence. Visual inspection of the promoter region of the *C. elegans nph-1* homolog revealed a close match with the consensus X-box located at position –77 in *C. briggsae* relative to the translational start site (Table 1). The putative X-box in the *nph-1* promoter was not identified in the *C. elegans* screen because of the presence of an additional nucleotide in the spacer region between the left and right half-sites of the X-box motif that was not permitted by the parameters of our search algorithm. While less common, a three-nucleotide spacer between the two X-box half-sites has been reported in several mammalian genes known to be regulated by the homologs of DAF-19 (Emery et al., 1996).

We also searched the *C. elegans* genome for the homologs of nephrocystin-2, nephrocystin-3 and nephrocystin-5. However, our analysis of the candidates indicated that any homology between *C. elegans* proteins and mammalian nephrocystin-2, nephrocystin-3 and nephrocystin-5 was restricted only to the ankyrin, TPR or IQ domains, respectively. Thus, we do not believe that the *C. elegans* genome encodes homologs of mammalian nephrocystin-2, nephrocystin-3 or nephrocystin-5.

The presence of putative X-box motifs in the promoters of *nph-1* and *nph-4* suggested that they would be expressed in ciliated sensory neurons of *C. elegans* and that further characterization of these genes would provide important insights into the mechanism by which cilia defects result in renal cystic diseases. In contrast to the ubiquitous nature of cilia in the mammalian body, cilia are found on only a subset of neurons (60 out of 302) in the head (amphid and labial) and tail (phasmid) of the *C. elegans* hermaphrodite, with the male containing an additional 52 ciliated neurons (Ward et al., 1975; Ware et al., 1975; White et al., 1986). To determine the expression patterns of *nph-1* and *nph-4*, we generated transcriptional fusion constructs consisting of the promoter region (300 bp up from the ATG) of *nph-1* fused with CFP (*nph-1::CFP*) or the promoter (1000 bp up from the ATG) of *nph-4* fused with DsRed2 (*nph-4::DsRed2*). Transgenic lines expressing these constructs were generated and the resulting expression patterns were compared to those of two known IFT genes (*osm-5* and *che-13*) (Haycraft et al., 2003; Haycraft et al., 2001). In agreement with the presence of an X-box motif, *nph-1* and *nph-4* expression was detected in most ciliated sensory neurons in the hermaphrodite (Figs 1 and 2). There was no expression of *nph-1* or *nph-4* evident in non-ciliated cell types. Overall, the expression pattern of *nph-1* was similar to that of the IFT genes (Fig. 2C). In the case of *nph-4*, we were able to generate only a single stable transgenic line. Analysis of this line shows *nph-4* expression in a subset of ciliated sensory neurons in the head of the worm as well as in most of the phasmid neurons in the tail. We do not believe that these data reflect the expression of the endogenous *nph-4* gene. This is based on the analysis of NPH-4 protein localization showing that it is expressed in a much broader spectrum of the ciliated neurons than seen using the transcriptional fusions and

Table 1. Conserved X-box sequences in *nph-1* and *nph-4* homologs

Species	Gene	Location*	X-box sequence†
C. elegans	*nph-1*(M28.7)	–77 to –63	**GTT**G**CC** **A**GG **GG**C**AAC**
C. briggsae	*nph-1*(CBG03043)	–68 to –55	**GTT**G**CC** **AT** **GG**T**CAC**
Mouse	*nephrocystin-1*	–14 to –1	**GTTTCC** C**T** **GA**C**AAC**
C. elegans	*nph-1*(R13h4.1)	–168 to –155	A**TTTCC** **AT** **GA**C**AAC**
C. briggsae	*nph-4*(CBG23249)	–186 to –173	A**TTTCC** **AT** **GG**C**AAC**
Mouse	nephrocystin-4	–231 to –218	**GTC**T**CC** TA **GG**T**AAC**
Consensus X-box (*C. elegans*)			**GTH**N**YY** **AT** **RR**N**AAC**

*For *C. elegans* and *C. briggsae* these positions are relative to the translational start site. The mouse positions are relative to the start of transcription.
†R=G/A; Y=C/T; H=A/T.C; N=G/A/T/C; bold letters denote a match to the *C. elegans* X-box consensus sequence.

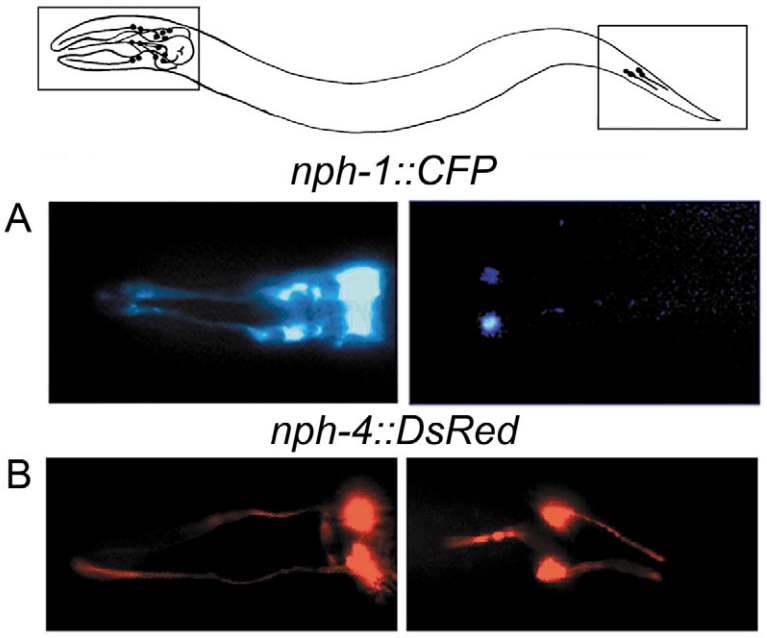

Fig. 1. Expression of *nph-1* and *nph-4* in *C. elegans*. (Top) Diagram showing the position of the neurons examined in A and B. (A) *nph-1::CFP* (L1 Stage) and (B) *nph-4::DsRed2* (adult) are expressed in the ciliated sensory neurons of the worm including the amphid and labial neurons in the head (left panels) as well as the phasmid neurons in the tail (right panels). In this figure and all following figures, anterior is toward the left.

on the recently published data of Wolf et al. indicating *nph-4* expression in most of the amphid and labial neurons (Wolf et al., 2005). The reason for this difference in expression and the difficulties in generating these stable lines is not known.

DAF-19 regulates expression of *nph-1* and *nph-4*

To assess the importance of the X-box sequences in the *nph-1* and *nph-4* promoters, we evaluated whether a similar motif was present in the homologs of these genes in other ciliated organisms. In *C. briggsae* a consensus X-box was present in the putative promoter regions of both *nph-1* and *nph-4*. The X-box motifs were located in nearly the identical positions relative to the start of translation of these genes in both organisms (Table 1). Comparison of the promoter regions outside the X-box sequence failed to show a high degree of conservation. Similarly, in the promoter regions of the mouse *nph-1* and *nph-4* homologs, a near consensus X-box sequence was identified located at position –14 for nephrocystin-1 and –231 for nephrocystin-4 relative to the start of transcription. Together these data suggest an evolutionarily conserved transcriptional regulatory mechanism controlling

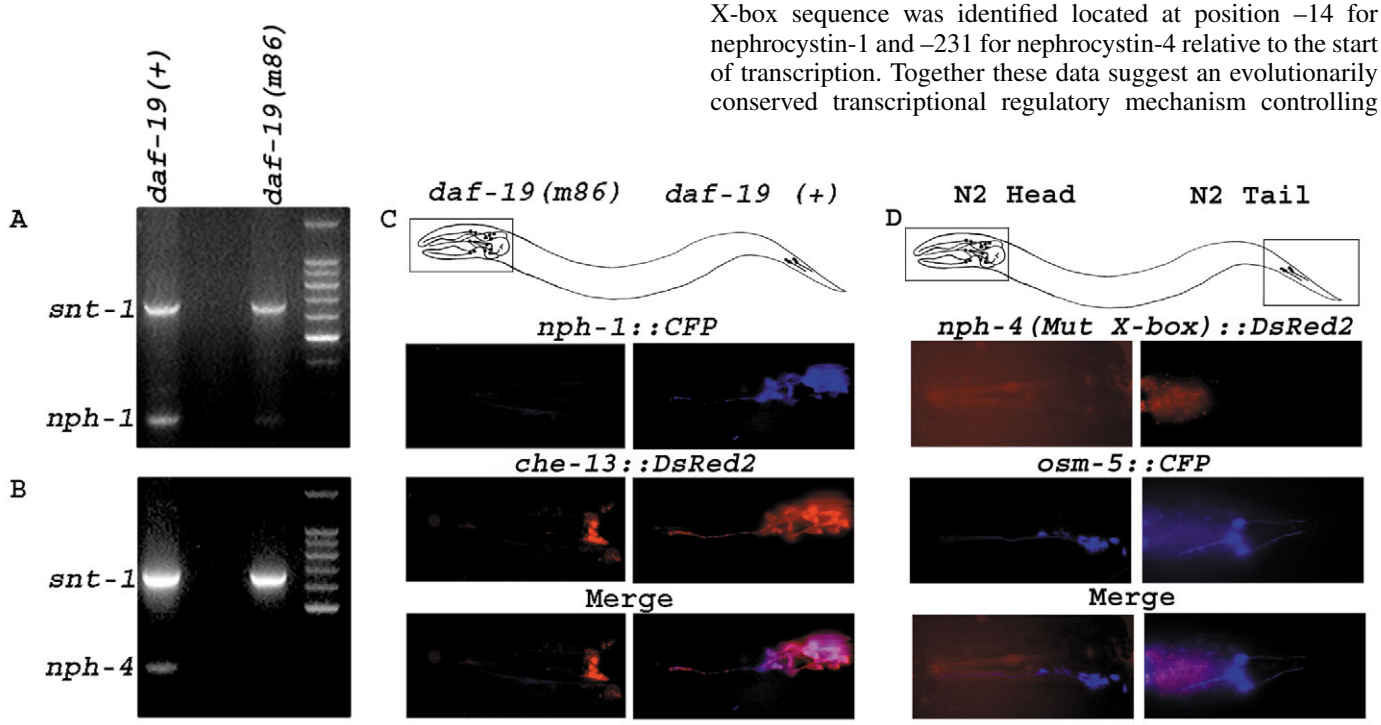

Fig. 2. DAF-19 regulation of *nph-1* and *nph-4*. RT-PCR analysis of (A) *nph-1* and (B) *nph-4* showed a marked decrease in expression of both genes in the *daf-19(m86)* mutant background compared to that seen in the *daf-19(+)* background. Synaptotagmin (*snt-1*) was used as a control for a neuronal gene whose expression is DAF-19 independent. (C) In vivo expression analysis of *nph-1::CFP* in *daf-19(m86)* mutant (left panels) and *daf-19(+)* (right panels) backgrounds. *nph-1::CFP* expression was greatly diminished in the *daf-19(m86)* background compared with *daf-19(+)*. A similar reduction in expression is seen for *che-13::DsRed2*, a gene encoding an IFT protein that is known to be regulated by DAF-19. The merged image of *nph-1::CFP* and *che-13::DsRed2* expression in the *daf-19 (+)* background shows that both of these genes are expressed in the same cells. (D) In vivo expression analysis in wild-type worms using the *nph-4(mut)::DsRed* transgene in which the X-box has been mutated. Mutation of the X-box results in the loss of *nph-4* expression in the ciliated sensory neurons relative to the same *nph-4* transgene with a wild-type X box (see Fig. 1B) or the IFT gene *osm-5::CFP* with wild-type X-box.

the expression of genes involved in cilia assembly and function that includes many of the IFT genes, several BBS genes, and now two genes involved in NPH (Efimenko et al., 2005).

To explore the potential importance of the X-box, we compared *nph-1* and *nph-4* expression levels in *daf-19(m86)* mutant and *daf-19*(+) backgrounds. This analysis was conducted using transgenic lines expressing the transcriptional fusion constructs, and by semi-quantitative RT-PCR to determine the effect on expression of the endogenous genes. RT-PCR analyses showed a significant decrease, but not complete abolition, of *nph-1* and *nph-4* expression in the *daf-19(m86)* mutant versus *daf-19(+)* backgrounds (Fig. 2A,B) whereas the expression level of the non-DAF-19 regulated neuronal gene synaptotagmin (*snt-1*) remained unchanged. Similarly, we detected a marked reduction in the expression of *nph-1::CFP* due to the loss of DAF-19 in transgenic worms (Fig. 2C). These results paralleled that of *che-13*, a known target for DAF-19 regulation (Haycraft et al., 2003). Finally, we generated transgenic worms that carry a mixed extrachromosomal array consisting of a *nph-4::DsRed2* transgene with a mutated X-box sequence and an *osm-5::CFP* transgene with a wild-type X-box. In contrast to the *osm-5::CFP*, which is expressed in ciliated sensory neurons, expression from the *nph-4(mut)::DsRed2* construct with the mutated X-box was not evident in any of the independent worms analyzed (*n*=18; Fig. 2D).

NPH-1 and NPH-4 localize to the base of cilia

Many of the genes whose expression is regulated by DAF-19 have been found to encode proteins that localize to cilia and are often involved in IFT and/or ciliogenesis. To determine if the *C. elegans* nephrocystins are cilia-associated proteins, we generated transgenic lines that co-expressed NPH-1 and NPH-4 as translational fusions with CFP and YFP, respectively. Analysis of multiple independent lines showed that NPH-1 and NPH-4 colocalize at the distal end of the dendrites of most, if not all, amphid, labial and phasmid neurons of the hermaphrodite and the sensory rays of the male tail (Fig. 3A and data not shown). This localization corresponds to the transition zone (analogous to the mammalian basal body) at the base of cilia as revealed by the analysis of transgenic worms coexpressing the NPH proteins along with the IFT protein CHE-13 (Fig. 3B,C, and see supplementary material, Fig. S1) (Haycraft et al., 2003). The transition zone is thought to be a site where cilia proteins concentrate and assemble into complexes prior to being

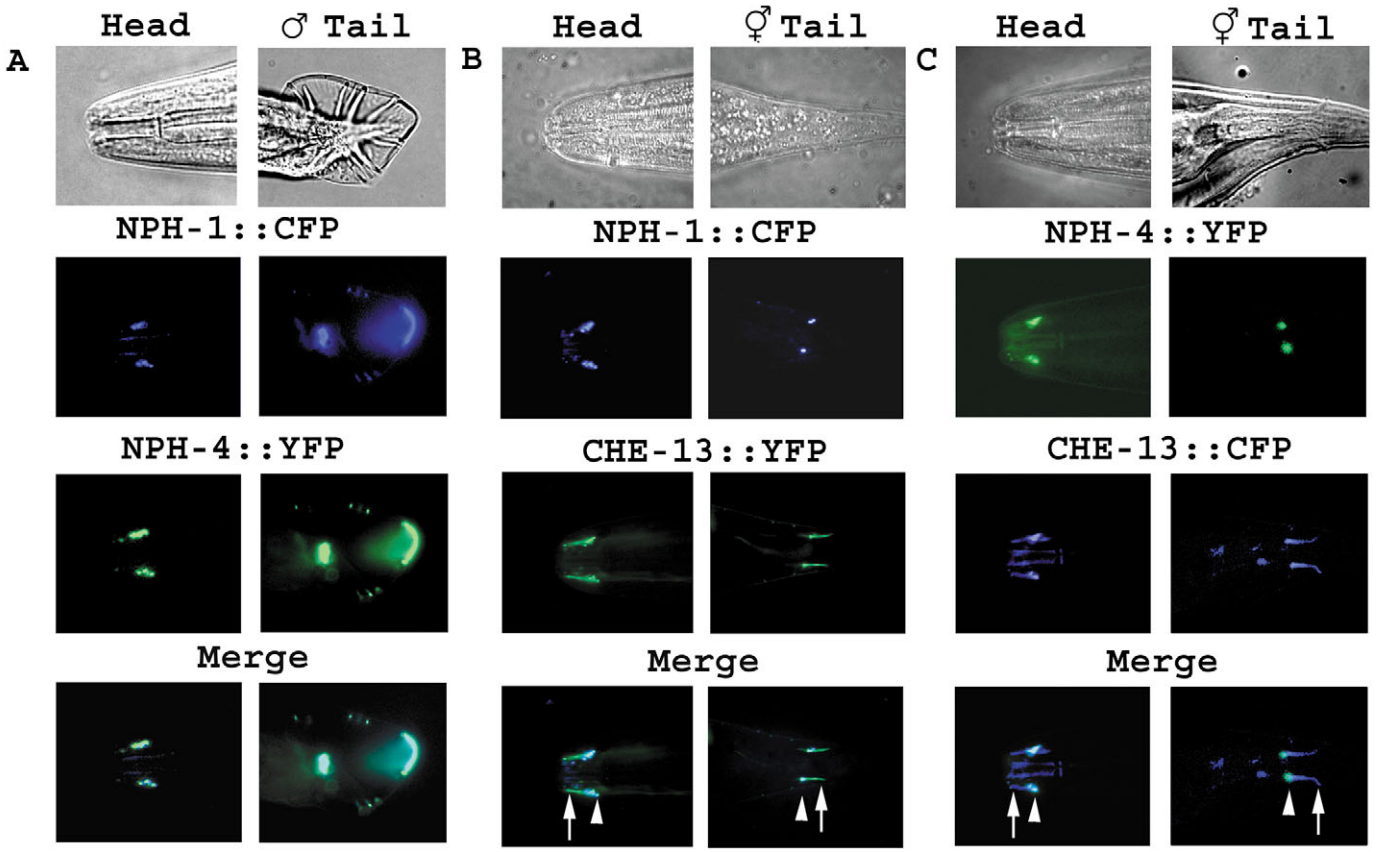

Fig. 3. Colocalization of the NPH-1 and NPH-4 proteins to the transition zone at the base of cilia in *C. elegans*. (A) Transgenic lines were generated that express NPH-1::CFP and NPH-4::YFP under control of their endogenous promoters. NPH-1 and NPH-4 colocalized to the distal end of the dendrites of the ciliated sensory amphid and labial neurons in the head of the worm (left panels) and the sensory rays of the male tail (right panels). (B,C) The localization of NPH-1 (B)and NPH-4 (C)was further evaluated by generating transgenic lines that co-express the IFT protein, CHE-13. CHE-13 was detected at the transition zones (arrowheads) and in the cilium axoneme (arrows); however, both NPH-1 and NPH-4 were restricted to the transition zone. There was no detectable signal for NPH-1 or NPH-4 in the axoneme. For enlarged images of the cilium region see Fig. S1 in supplementary material.

transported into the cilium axoneme (Scholey, 2003). However, in contrast to the characterized IFT and BBS proteins, analysis of NPH-4::YFP and NPH-1::CFP failed to show any localization of the fusion proteins within the cilium axoneme even with increased exposure during image acquisition.

Characterization of *nph-1* and *nph-4* mutant alleles

To begin analyzing the function of the NPH proteins at the transition zone, we obtained RB743 *nph-1*(*ok500*) and FX925 *nph-4*(*tm925*) mutant strains from the *C. elegans* Knockout Consortium and the National BioResource Project (Japan), respectively. Sequence analysis of the *nph-1* genomic region isolated from *nph-1(ok500)* mutants indicates a deletion that begins in intron 5 and extends into the terminal exon, thus deleting exon 6 through to the beginning of exon 9. If expressed, the mutant protein would lack C-terminal amino acids after residue 358 including much of the nephrocystin homology domain, but would retain the SH3 domain in the N terminus (Fig. 4). Importantly, this mutation would delete much of the region that in mammalian nephrocystin-1 is thought to directly interact with the nephrocystin-4 protein (Mollet et al., 2005).

The *nph-4*(*tm925*) mutation is an intragenic deletion that begins in intron 2 and extends into intron 6, deleting amino acids 86-264 out of the total 1305 (Fig. 4). While NPH-4 has no well-characterized motifs, this mutation does delete a highly conserved sequence found in human, mouse, *C. elegans C. briggsae* and *Xenopus tropicalis* homologs, suggesting its functional importance. In addition, the mutation would remove a majority of the region thought to mediate the interaction of nephrocystin-4 with nephrocystin-1 (Mollet et al., 2005).

To better characterize these mutations, we analyzed the expression of *nph-1* and *nph-4* in the corresponding mutant by RT-PCR. The data indicate that in both mutants there is abnormal splicing of the mutated transcripts that results in two variants in *nph-1(ok500)* mutants and three variants in *nph-4(tm925)* mutants (see supplementary material, Fig. S2). Sequence analyses of the products in the *nph-1(ok500)* mutants indicate that both variants delete most of the nephrocystin homology domain (NHD) and result in reading frame shifts and with early truncation of the protein. The abnormal splice variants in *nph-4(tm925)* mutants all cause changes in the reading frame and result in early termination of the protein with the largest protein being 107 amino acids out of 1,305. Therefore it is probable that these mutations represent null alleles. Additionally in both mutants, the deletions affect regions important for formation of the NPH complex (Mollet et al., 2005).

Cilia formation is normal in *nph* mutants

To begin characterizing the phenotypes associated with mutations in the *nph* genes, we assessed whether the *nph-1*, *nph-4*, or *nph-1;nph-4* double mutants exhibited any abnormalities associated with ciliogenesis or cilia morphology. In *C. elegans*, the amphid and phasmid neurons, which express *nph-1* and *nph-4*, extend cilia through the cuticle where they can absorb fluorescent hydrophobic dye in the medium (Starich et al., 1995). In contrast, *C. elegans* with cilia assembly defects (such as the IFT mutants) are unable to absorb dye (Dyf phenotype). Our results from the dye-filling assay indicate that there are no major morphological abnormalities in the cilia as seen in *osm-5* or *che-13* IFT mutants since both the single and the double *nph* mutants absorb fluorescent dye identically to that seen in the N2 wild-type controls (Fig. 5A) (Haycraft et al., 2003; Haycraft et al., 2001). However, it should be noted that there are IFT mutants (i.e. several of the complex A mutants or *klp-11* and *kap-1*) that do not or only partially dye-fill (Starich et al., 1995; Perkins et al., 1986; Snow et al., 2004). Thus, to further evaluate possible defects in cilia structure, we generated *nph-1/nph-4* double mutants expressing the cilia marker CHE-13 fused to YFP and measured the length of the cilia on the amphid and phasmid neurons. The data indicate that there are no overt differences in cilia length in the double mutant relative to wild-type controls (Fig. 5B,C).

nph mutants exhibit defects in chemotaxis and lifespan regulation

In *C. elegans*, cilia on the amphid and phasmid neurons play important roles in sensory perception that allow the worm to

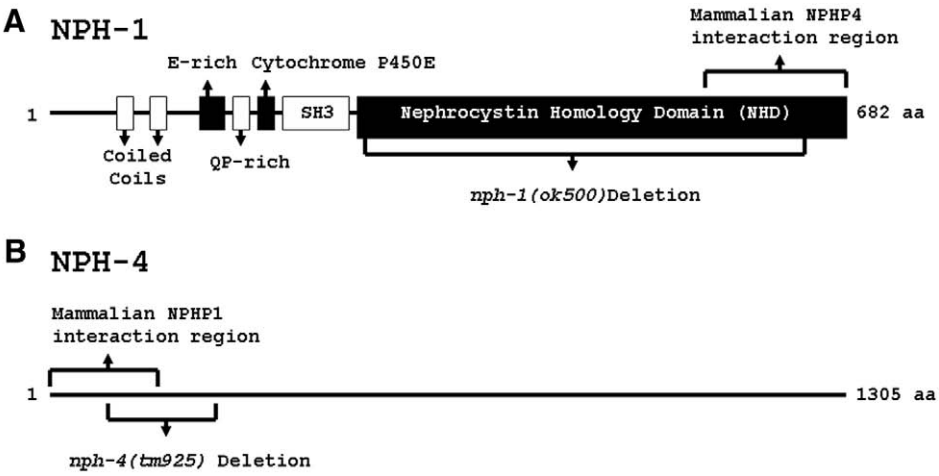

Fig. 4. *C. elegans* NPH-1 and NPH-4 protein domain structures. (A) The *C. elegans* NPH-1 protein consists of two coiled-coil domains, an E-rich domain, a QP-rich domain (glutamate-proline rich domain), cytochrome P450E, an SH3 domain, and the nephrocystin homology domain (NHD). The deleted region (amino acids 281-641) in the *nph-1(ok500)* mutant is indicated as well as the nephrocystin-4 mammalian interaction region (C-terminal 131 amino acids). The protein sequence is based on the mRNA sequence derived from NM_063897. (B) The NPH-4 protein in *C. elegans* does not exhibit any well-characterized domains. The deletion, which spans amino acids 86-264 in *nph-4(tm925)* mutants, and the region involved in the interaction with mammalian nephrocystin-1 (N-terminal 176 amino acids) are indicated. The protein sequence is based on the mRNA sequence from AY959881.

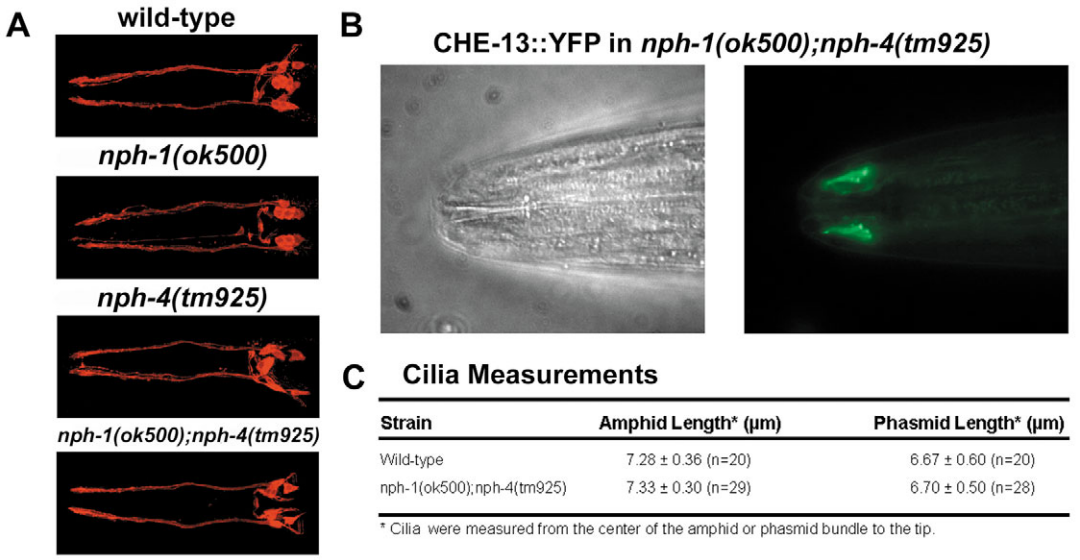

Fig. 5. Cilium structure analysis of *nph-1;nph-4* double mutants. (A) Cilium structure was analyzed by evaluating the ability of *nph-1*, *nph-4* and double *nph-1;nph-4* mutants to absorb DiI (dye-filling assay). There were no overt differences detected between any of the mutant strains when compared to that of wild-type controls. (B) Cilium structure was further analyzed in *nph-1;nph-4* double mutants using the CHE-13::YFP fusion protein. Cilium structure was indistinguishable from that of wild-type controls and CHE-13::YFP was properly localized throughout the cilium. (C) To evaluate possible effects of the *nph* mutants on cilium structure, the length of cilia was determined in *nph-1;nph-4* double mutants expressing CHE-13::YFP. There were no statistically significant differences detected in the cilia of wild type and double mutant lines. Identical results were obtained with *nph-4* single mutants (data not shown).

evaluate its surroundings. Despite normal cilia, the *nph-1; nph4* double mutant males have been shown to be defective in mating response and Wolf et al. showed pronounced defects in mating efficiency in both single mutants using RNAi knockdown approaches (Wolf et al., 2005; Jauregui and Barr, 2005). To further assess whether the *nph* mutant hermaphrodites have abnormalities in cilia-mediated sensory functions, we assayed whether the mutants have defects in dauer formation, osmotic avoidance, lifespan regulation and chemotaxis.

The dauer larva is a protective stage of the *C. elegans* life cycle brought on by stressful conditions (Golden and Riddle, 1984; Starich et al., 1995). It can be induced by pheromones released in response to lack of food or overcrowding, which are thought to be perceived by the ciliated sensory neurons. To evaluate the effect of *nph* mutations on dauer formation, wild-type worms, *nph-1*, *nph-4* single mutants, *nph-1;nph-4* double mutants, and *osm-5* mutants were starved to induce dauer formation and then treated with 1% SDS solution. Dauers are able to survive SDS treatment and can re-enter the life cycle when plated on bacterial lawns. As shown previously, the *osm-5* mutants are unable to form dauer larvae in response to starvation and no viable animals were obtained after SDS treatment. In contrast, wild-type *C. elegans* and *nph* mutants under the same conditions produced numerous dauer stage larvae indicating that *nph-1* and *nph-4* are not required for dauer formation (data not shown).

The cilia on sensory neurons that extend through the cuticle of *C. elegans* are also important in sensing osmotic concentrations. Wild-type N2 worms are able to sense regions of high osmolarity and exhibit an avoidance behavior, while IFT mutants are defective in osmotic avoidance (Osm phenotype). To determine if the loss of the NPH proteins results in an Osm phenotype, we placed a ring of 4 M NaCl or 8 M glycerol on plates and mutant or wild-type worms were placed in the center of the ring. Worms that were unable to sense the osmotic concentration, such as the *osm-5* or *che-13* IFT mutants, migrated freely into and across the ring. In contrast, the *nph* mutant worms avoided the high osmotic zones similar to the wild-type controls, suggesting that *nph-1* and *nph-4* are not required for osmotic avoidance (data not shown).

Cilia-mediated sensory reception is also thought to influence lifespan in *C. elegans* (Apfeld and Kenyon, 1999). This is supported by the fact that many of the IFT mutants, such as *osm-5*, have a marked increase in lifespan. Although the role that cilia play in this process remains elusive, it has been proposed that lifespan in *C. elegans* is regulated in part by receptors located in the cilia that receive environmental signals. To determine whether the NPH proteins play a role in this process, *nph-1*, *nph-4*, *nph-1;nph-4* and *osm-5* mutants and wild-type N2 control worms were synchronized and their survival was followed daily. The single *nph-1* and *nph-1;nph-4* double mutant exhibited an extension in lifespan compared with the wild-type controls (Fig. 6); however, the extension was not as dramatic as seen in the *osm-5* IFT mutant. Interestingly, *nph-4* single mutants have a lifespan similar to that of the *osm-5* mutants. In all three independent lifespan assays conducted, the *nph-4* mutation had a more severe effect on lifespan than did the double *nph-1;nph-4* mutations. The reason for the more severe phenotype in *nph-4* mutants is uncertain; however, we suspect that it indicates that NPH-4 has a role in regulating NPH-1 function. In the absence of NPH-4, NPH-1 would exhibit aberrant activity that could lead to the more severe phenotype. This aberrant NPH-1 activity would

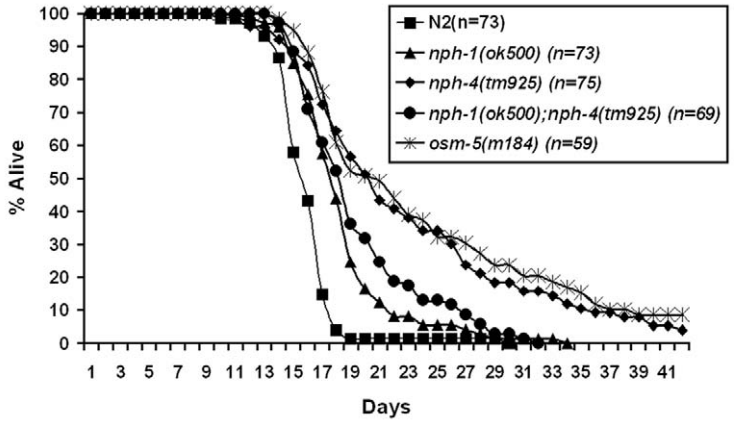

Fig. 6. Lifespan analysis of *nph-1* and *nph-4* single and double mutants in *C. elegans*. The lifespan of *nph-1*, *nph-4* and *nph-1;nph-4* double mutants was compared to N2 wild-type controls and the long lived *osm*-5 cilia mutants. The *nph-1(ok500)*, *nph-4(tm925)* and *nph-1(ok500); nph-4(tm925)* double mutant strains had a significant expansion in lifespan compared to the N2 worms. Although the *nph-1(ok500)* and *nph-1(ok500); nph-4(tm925)* double mutants did not have as severe of an increase in lifespan as *osm-5* mutant worms, single *nph-4(tm925)* mutants were indistinguishable from *osm*-5 mutant worms. Similar data were obtained on three independent lifespan experiments (average of 75 total worms in each genetic category) conducted for this analysis.

then be removed in the *nph-1;nph-4* double mutants resulting in a less severe phenotype. We are currently exploring this possibility.

To further explore the possible connection between the NPH proteins and sensory perception, we tested whether loss of the NPH proteins altered the response of mutant worms to the volatile chemoattractants benzaldehyde and diacetyl that are perceived by two separate classes of neurons, the AWC and AWA neurons, respectively (Sengupta et al., 1996; Wes and Bargmann, 2001). Using standard chemotaxis assays (Bargmann et al., 1993; Blacque et al., 2004), we found that the majority of the wild-type N2 worms respond chemotactically and move into the attractant zone within 30 minutes of placing the worms on the chemotaxis plates. In addition, the path by which the N2 worms migrate is relatively unidirectional toward the source of the attractant. In contrast to the N2 controls, *nph-1*, *nph-4* and the *nph-1;nhp-4* double mutants exhibited a significant delay in their chemotaxis response toward both attractants (Fig. 7A,B). While many of the mutant worms do eventually reach their destination at the attractant, the migration path was less unidirectional than that of the N2 control worms and was typical of mutants with sensory defects associated with loss of cilia function (Starich et al., 1995). Importantly, in both mutant lines the chemotaxis defects were corrected by expression of the respective wild-type *nph* gene (Fig. 7A,B).

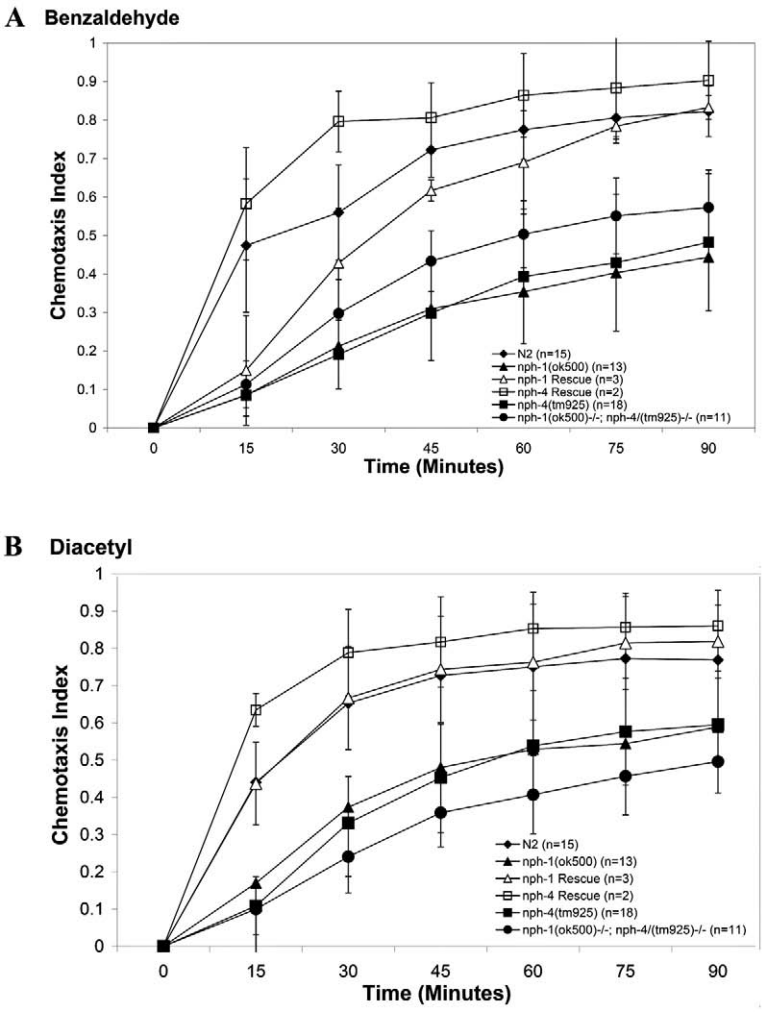

NPH-4 is required for NPH-1 localization to the transition zone

The mammalian nephrocystin proteins are thought to function in the same pathway and there is data to suggest a physical interaction between several of the NPH proteins (Mollet et al., 2002; Mollet et al., 2005). The specific chemotaxis and lifespan defects in the absence of cilia structure abnormalities in the

Fig. 7. The *nph-1* and *nph-4* single and *nph-1;nph-4* double mutants exhibit defects in chemotaxis toward volatile attractants. Comparison of chemotaxis indices for the wild-type N2 and the *nph* mutants in response to (A) benzaldehyde and (B) diacetyl indicate that both single mutants and the double mutant exhibit abnormal response to these attractants. To demonstrate that the phenotypes were the result of mutation of the *nph* genes, the chemotaxis defect in *nph-1* and *nph-4* mutants was rescued by expression of *nph-1::CFP* and *nph-4::YFP*, respectively. Both the *nph-1* and *nph-4* rescued lines exhibited a strong chemotactic response to (A) benzaldehyde or (B) diacetyl similar to that obtained for wild-type controls. Error bars represent the standard deviation and *n* refers to the number of independent experiments with an average of 100 worms on each plate being evaluated.

nph-1 and *nph-4* mutants also support this conclusion in *C. elegans*. To obtain further insight into this possibility, we analyzed the effect of each *nph* mutation on the localization of the reciprocal NPH protein. In *nph-1* mutants, NPH-4 localization at the transition zones was unchanged from that in wild-type controls (Fig. 8A). In contrast, NPH-1 was not localized to the transition zone in the *nph-4* mutants (Fig. 8B). Passing the NPH-1::CFP extrachromosomal array from the *nph-4* mutants onto a wild-type background restored NPH-1 localization to the transition zone (Fig. 8C). In addition, *nph-1* expression is maintained in the *nph-4* mutants (data not shown), thus indicating that NPH-4 function is required for normal localization of NPH-1 to the transition zone, and supporting the concept that the NPH proteins function as part of the same complex.

Discussion

The development of renal cysts is common to a number of human and murine disorders including autosomal recessive (ARPKD), autosomal dominant polycystic kidney disease (ADPKD), nephronophthisis (NPH), Bardet-Biedl Syndrome (BBS) and oral facial digital syndrome (OFD) (Ansley et al., 2003; Romio et al., 2004; Wilson, 2004). The identification of several genes associated with the pathologies in these disorders has revealed that a unifying cause may be an association with defects in cilia assembly or cilia-mediated functions. However, the role of most of these 'ciliocystic' proteins and the spectrum of functions of renal cilia remains largely unsolved. Currently it is believed that renal cilia function as mechanosensors that evaluate changes in fluid flow through the lumen (Praetorius and Spring, 2001; Praetorius and Spring, 2003). Deflection of the cilium axoneme initiates an increase in intracellular calcium which requires the polycystins, the proteins that are disrupted in human ADPKD (Nauli et al., 2003).

To further understand the connection between cilia and renal cyst development, we have utilized *C. elegans* as a malleable system to facilitate functional analysis of ciliocystic proteins. As part of these analyses, we conducted a nematode genome sequence-based screen to identify genes expressed in the sensory cilia. The basis of the screen was the co-regulation of several cilia genes by DAF-19 (Efimenko et al., 2005; Swoboda et al., 2000). Among the candidate genes were several IFT proteins, homologs of genes involved in human Bardet-Biedl Syndrome, as well as the homologs of nephrocystin-1 and nephrocystin-4. Thus, we speculated that the *nph* genes would encode cilia-associated proteins and that NPH would represent another model system to evaluate cilia dysfunction and renal cystic disease.

Our initial characterization of *nph-1* and *nph-4* confirmed that both genes are regulated by DAF-19 in agreement with the presence of an X-box in the promoter region and that they are expressed in ciliated sensory neurons of both the male and hermaphrodite. The presence of an X-box sequence in the promoters of these genes in the related nematode *C. briggsae* and in the putative promoter regions of nephrocystin-1 and nephrocystin-4 in the mouse argues that this motif is functional in these genes. We confirmed this in the case of *nph-4* by mutating the X-box sequence and demonstrating a marked reduction in expression from the transgene. In addition, the expression pattern of *nph-1* and *nph-4* shown here and previously by Wolf et al. and Jauregui and Barr is similar to that seen for DAF-19-regulated IFT genes such as *osm-5* or *che-13* (Haycraft et al., 2003; Haycraft et al., 2001) and the recently described *bbs-1*, *bbs-2*, *bbs-5*, *bbs-7* and *bbs-8* (Blacque et al., 2004; Li et al., 2004; Efimenko et al., 2005). However, in contrast to OSM-5, CHE-13, BBS-7 and BBS-8, the NPH proteins were not detectable in the cilium axoneme at this level of analysis. Rather, NPH-1 and NPH-4 remained at the transition zones at the base of the cilia. We know that the extrachromosomal arrays used to conduct these localization studies encode functional proteins since they are able to rescue the mutant chemotaxis phenotypes. In addition, our data indicate that *nph-1* and *nph-4*, are distinct from the IFT proteins and most of the BBS proteins in that the *nph* mutants show no gross abnormalities in cilia morphology. Thus, from

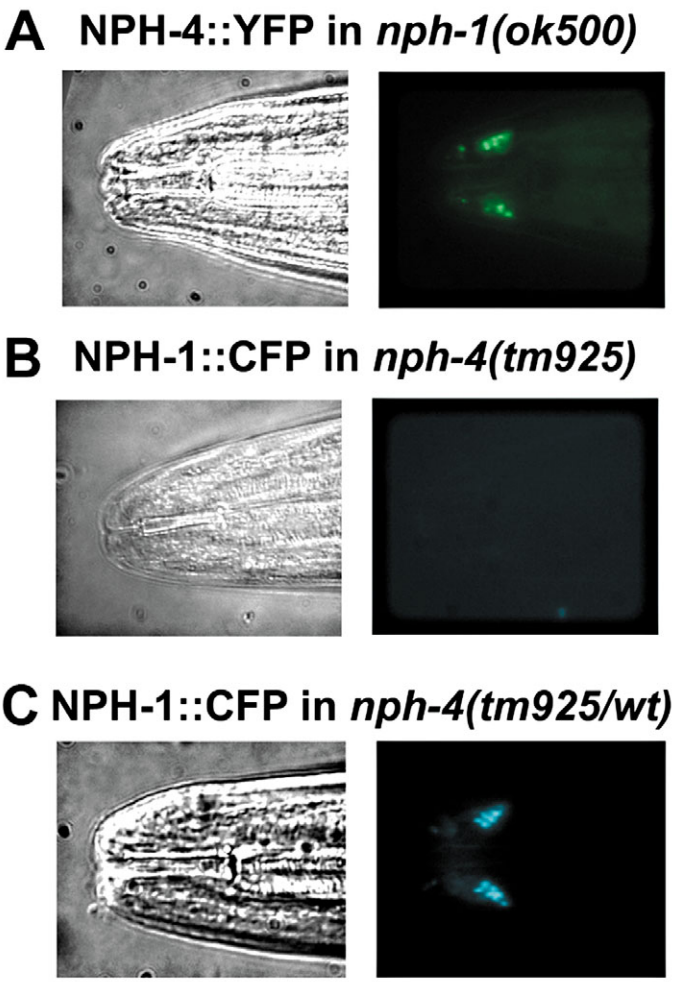

Fig. 8. The NPH-4 protein is required for proper localization of NPH-1 to the transition zone. To explore the possibility that the NPH proteins function as part of the same complex, we analyzed the localization of the NPH proteins in the reciprocal mutant background. (A) Compared to wild-type controls, NPH-4::YFP localization was not altered by loss of *nph-1*. (B) In contrast, NPH-1::CFP was not detected at the transition zone in *nph-4* mutants indicating that NPH-4 is required for NPH-1 localization. (C) The localization of NPH-1::CFP to the transition zone was restored by crossing the strain back to wild-type worms.

these data it seems unlikely that the *C. elegans* NPH proteins have a role in cilia assembly as proposed recently by Wolf et al. (Wolf et al., 2005).

Characterization of the first four mammalian nephrocystins has suggested that they form a complex and function in a common signaling pathway (Mollet et al., 2005; Olbrich et al., 2003; Otto et al., 2003). Despite the lack of clear homologs to nephrocystin-2 and nephrocystin-3 in *C. elegans*, our data further support this conclusion based on the similar sensory defects observed with the single and double *nph* mutants in *C. elegans* and from the mislocalization of NPH-1 protein in *nph-4* mutants. The latter data also suggests that one function of NPH-4 is to anchor NPH-1 at the transition zones. This is supported further by recent data in *Chlamydomonas* identifying the NPH-4 protein, but not NPH-1, as a central component of the centriole that forms the basal body from which the flagella emerges (Keller et al., 2005). Since homologs of the additional nephrocystins do not appear to be in the *C. elegans* genome, we are unable to test the effects of *nph-4* mutation on their localization; however, we are utilizing the power of the *C. elegans* model system to screen for additional proteins that may function as part of the NPH complex and may provide novel insights into the function of the mammalian proteins.

Despite the lack of any morphological defect in the cilia, our analyses of the *nph* mutants reveal that they exhibit phenotypes typical of mutants with defects in cilia-mediated signaling. Although osmotic avoidance and dauer formation were overtly normal, the *nph* mutants did exhibit an increase in lifespan as well as abnormalities in chemotaxis toward two volatile chemoattractants. The effects in the *nph-1* and *nph-1;nph-4* double mutants were not as pronounced as those reported for a typical cilia assembly mutant, such as *osm-5*, but were significantly different from wild-type controls. In contrast, mutation of *nph-4* was found to have a more severe effect on lifespan. Although we do not know the reason for the more severe phenotype in the *nph-4* mutant than in the *nph-1;nph-4* double mutants, a possibility is that the NPH proteins have a role in regulating each others' functions. This is supported by the dependence of NPH-1 on NPH-4 for localization to the transition zone. Thus, in the *nph-4* mutants, NPH-1 may be free from regulatory influences normally provided by NPH-4 and lead to a more severe phenotype, which is then removed in the case of the double mutants. Additionally, NPH-1 could act genetically downstream of *nph-4* in the *nph* pathway and suppress aspects of the *nph-4* mutant phenotype in the *nph-1; nph-4* double mutant worms. Studies to address these issues are currently underway.

In contrast to the effect on lifespan, we detected no consistent differences between the single and double mutants with regards to their chemotactic response toward volatile attractants. The reason for this is unknown but may indicate that these proteins have slightly different roles in these sensory responses or in different neurons involved in chemotaxis and lifespan regulation.

It has recently been demonstrated that RNAi-mediated knockdown of *nph-1* or *nph-4* results in a male mating defect reminiscent of *lov-1* and *pkd-2* mutants (Wolf et al., 2005). Additionally, Jauregui and Barr have shown that the *nph-1; nph-4* double mutants, but not single mutants, have defects in the response step of male mating (Jauregui and Barr, 2005). The reason for the discrepancy in the mating phenotype between the genetic mutants and the knockdowns is unknown. It is surprising that the phenotype is more severe in the knockdown mutants since RNAi approaches are notoriously ineffective in neurons in *C. elegans*. The male mating defects along with our data indicating that *nph* mutants have abnormalities in chemotaxis and lifespan support a role for NPH proteins as regulators of signaling activity mediated by cilia on the sensory neurons.

Since the cilia in *nph* mutants appear normal, it will be interesting to determine whether disruption of the NPH proteins affects localization or transport of chemoreceptors or channels within the cilia such as *odr-10*, which mediates responses to diacetyl (Sengupta et al., 1996), or *pkd-2*, which is involved in male mating. Alternatively, loss of NPH proteins may disrupt events downstream from these receptors or channels and may be involved in transmission of the cilia-mediated signaling to the cell body. In support of these possibilities, it has recently been found that X-box-containing genes can be divided into two separate groups depending upon their X-box sequence relationship to the consensus and to the distance of the X-box relative to the ATG. Based on these criteria, the *nph* genes can be classified as group 2 X-box genes that are thought to perform more specialized sensory functions, in contrast to group 1 genes that are hypothesized to be involved in cilia assembly (Efimenko et al., 2005). While the exact role of the NPH proteins in cilia remains elusive, *C. elegans* and the powerful genetic approaches afforded by this system will provide an important research tool to begin evaluating these possibilities and lead to a better understanding of the functions of renal cilia and how defects in this organelle lead to the formation of cysts in the kidney.

We gratefully acknowledge L. Guay-Woodford for critical reading of this manuscript. We thank A. Fire for the gifts of *C. elegans* expression vectors and S. Clark for the UNC-122::GFP construct. The *C. elegans* Genome Sequencing Consortium provided sequence information and the *Caenorhabditis* Genetics Center, which is funded by the National Institutes of Health, provided some of the *C. elegans* strains used in this study. We thank the *C. elegans* Knockout Consortium and the National BioResource Project in Japan for providing the *nph-1* and *nph-4* deletion mutants. This work was supported by grants to B.K.Y. from the National Institute of Diabetes and Digestive and Kidney Diseases, grants DK65655 and DK62758 and by a grant to P.S. from the Swedish Foundation for Strategic Research (SSF) in Stockholm, Sweden. Additional support was provided by NIH training grants DK07545 (C.J.H.) and 5 T32 GM008111(J.C.S.).

References

Ansley, S. J., Badano, J. L., Blacque, O. E., Hill, J., Hoskins, B. E., Leitch, C. C., Kim, J. C., Ross, A. J., Eichers, E. R. and Teslovich, T. M. (2003). Basal body dysfunction is a likely cause of pleiotropic Bardet-Biedl syndrome. *Nature* **425**, 628-633.

Apfeld, J. and Kenyon, C. (1999). Regulation of lifespan by sensory perception in Caenorhabditis elegans. *Nature* **402**, 804-809.

Bargmann, C. I., Hartwieg, E. and Horvitz, H. R. (1993). Odorant-selective genes and neurons mediate olfaction in C. elegans. *Cell* **74**, 515-527.

Barr, M. M., DeModena, J., Braun, D., Nguyen, C. Q., Hall, D. H. and Sternberg, P. W. (2001). The Caenorhabditis elegans autosomal dominant polycystic kidney disease gene homologs lov-1 and pkd-2 act in the same pathway. *Curr. Biol.* **11**, 1341-1346.

Benzing, T., Gerke, P., Hopker, K., Hildebrandt, F., Kim, E. and Walz, G. (2001). Nephrocystin interacts with Pyk2, p130(Cas), and tensin and

triggers phosphorylation of Pyk2. *Proc. Natl. Acad. Sci. USA* **98**, 9784-9789.

Blacque, O. E., Reardon, M. J., Li, C., McCarthy, J., Mahjoub, M. R., Ansley, S. J., Badano, J. L., Mah, A. K., Beales, P. L., Davidson, W. S. et al. (2004). Loss of C. elegans BBS-7 and BBS-8 protein function results in cilia defects and compromised intraflagellar transport. *Genes Dev.* **18**, 1630-1642.

Brenner, S. (1974). The genetics of Caenorhabditis elegans. *Genetics* **77**, 71-94.

Donaldson, J. C., Dempsey, P. J., Reddy, S., Bouton, A. H., Coffey, R. J. and Hanks, S. K. (2000). Crk-associated substrate p130(Cas) interacts with nephrocystin and both proteins localize to cell-cell contacts of polarized epithelial cells. *Exp. Cell Res.* **256**, 168-178.

Donaldson, J. C., Dise, R. S., Ritchie, M. D. and Hanks, S. K. (2002). Nephrocystin-conserved domains involved in targeting to epithelial cell-cell junctions, interaction with filamins, and establishing cell polarity. *J. Biol. Chem.* **277**, 29028-29035.

Dorman, J. B., Albinder, B., Shroyer, T. and Kenyon, C. (1995). The age-1 and daf-2 genes function in a common pathway to control the lifespan of Caenorhabditis elegans. *Genetics* **141**, 1399-1406.

Efimenko, E., Bubb, K., Mak, H. Y., Holzman, T., Leroux, M. R., Ruvkun, G., Thomas, J. H. and Swoboda, P. (2005). Analysis of *xbx* genes in *C. elegans*. *Development* **132**, 1923-1934.

Emery, P., Strubin, M., Hofmann, K., Bucher, P., Mach, B. and Reith, W. (1996). A consensus motif in the RFX DNA binding domain and binding domain mutants with altered specificity. *Mol. Cell. Biol.* **16**, 4486-4494.

Gandhi, S., Santelli, J., Mitchell, D. H., Stiles, J. W. and Sanadi, D. R. (1980). A simple method for maintaining large, aging populations of Caenorhabditis elegans. *Mech. Ageing Dev.* **12**, 137-150.

Golden, J. W. and Riddle, D. L. (1984). The Caenorhabditis elegans dauer larva: developmental effects of pheromone, food, and temperature. *Dev. Biol.* **102**, 368-378.

Haycraft, C. J., Swoboda, P., Taulman, P. D., Thomas, J. H. and Yoder, B. K. (2001). The *C. elegans* homolog of the murine cystic kidney disease gene Tg737 functions in a ciliogenic pathway and is disrupted in *osm-5* mutant worms. *Development* **128**, 1493-1505.

Haycraft, C. J., Schafer, J. C., Zhang, Q., Taulman, P. D. and Yoder, B. K. (2003). Identification of CHE-13, a novel intraflagellar transport protein required for cilia formation. *Exp. Cell Res.* **284**, 251-263.

Hildebrandt, F. and Otto, E. (2000). Molecular genetics of nephronophthisis and medullary cystic kidney disease. *J. Am. Soc. Nephrol.* **11**, 1753-1761.

Hildebrandt, F. and Omram, H. (2001). New insights: nephronophthisis-medullary cystic kidney disease. *Pediatr. Nephrol.* **16**, 168-176.

Jauregui, A. R. and Barr, M. M. (2005). Functional characterization of the C. elegans nephrocystins NPHP-1 and NPHP-4 and their role in cilia and male sensory behaviors. *Exp. Cell Res.* **305**, 333-342.

Keller, L. C., Romijn, E. P., Zamora, I., Yates, J. R., 3rd and Marshall, W. F. (2005). Proteomic analysis of isolated chlamydomonas centrioles reveals orthologs of ciliary-disease genes. *Curr. Biol.* **15**, 1090-1098.

Kozminski, K. G., Johnson, K. A., Forscher, P. and Rosenbaum, J. L. (1993). A motility in the eukaryotic flagellum unrelated to flagellar beating. *Proc. Natl. Acad. Sci. USA* **90**, 5519-5523.

Li, J. B., Gerdes, J. M., Haycraft, C. J., Fan, Y., Teslovich, T. M., May-Simera, H., Li, H., Blacque, O. E., Li, L., Leitch, C. C. et al. (2004). Comparative genomics identifies a flagellar and basal body proteome that includes the BBS5 human disease gene. *Cell* **117**, 541-552.

Loria, P. M., Hodgkin, J. and Hobert, O. (2004). A conserved postsynaptic transmembrane protein affecting neuromuscular signaling in Caenorhabditis elegans. *J. Neurosci.* **24**, 2191-2201.

Matsuura, T., Oikawa, T., Wakabayashi, T. and Shingai, R. (2004). Effect of simultaneous presentation of multiple attractants on chemotactic response of the nematode Caenorhabditis elegans. *Neurosci. Res.* **48**, 419-429.

Mello, C. C., Kramer, J. M., Stinchcomb, D. and Ambros, V. (1991). Efficient gene transfer in C.elegans: extrachromosomal maintenance and integration of transforming sequences. *EMBO J.* **10**, 3959-3970.

Mollet, G., Salomon, R., Gribouval, O., Silbermann, F., Bacq, D., Landthaler, G., Milford, D., Nayir, A., Rizzoni, G., Antignac, C. et al. (2002). The gene mutated in juvenile nephronophthisis type 4 encodes a novel protein that interacts with nephrocystin. *Nat. Genet.* **32**, 300-305.

Mollet, G., Silbermann, F., Delous, M., Salomon, R., Antignac, C. and Saunier, S. (2005). Characterization of the nephrocystin/nephrocystin-4 complex and subcellular localization of nephrocystin-4 to primary cilia and centrosomes. *Hum. Mol. Genet.* **14**, 645-656.

Murcia, N. S., Richards, W. G., Yoder, B. K., Mucenski, M. L., Dunlap, J. R. and Woychik, R. P. (2000). The Oak Ridge Polycystic Kidney (orpk) disease gene is required for left-right axis determination. *Development* **127**, 2347-2355.

Nauli, S. M., Alenghat, F. J., Luo, Y., Williams, E., Vassilev, P., Li, X., Elia, A. E., Lu, W., Brown, E. M., Quinn, S. J. et al. (2003). Polycystins 1 and 2 mediate mechanosensation in the primary cilium of kidney cells. *Nat. Genet.* **33**, 113-114.

Olbrich, H., Fliegauf, M., Hoefele, J., Kispert, A., Otto, E., Volz, A., Wolf, M. T., Sasmaz, G., Trauer, U., Reinhardt, R. et al. (2003). Mutations in a novel gene, NPHP3, cause adolescent nephronophthisis, tapeto-retinal degeneration and hepatic fibrosis. *Nat. Genet.* **34**, 455-459.

Otto, E., Kispert, A., Schatzle Lescher, B., Rensing, C. and Hildebrandt, F. (2000). Nephrocystin: gene expression and sequence conservation between human, mouse, and Caenorhabditis elegans. *J. Am. Soc. Nephrol.* **11**, 270-282.

Otto, E., Hoefele, J., Ruf, R., Mueller, A. M., Hiller, K. S., Wolf, M. T., Schuermann, M. J., Becker, A., Birkenhager, R., Sudbrak, R. et al. (2002). A gene mutated in nephronophthisis and retinitis pigmentosa encodes a novel protein, nephroretinin, conserved in evolution. *Am. J. Hum. Genet.* **71**, 1161-1167.

Otto, E. A., Schermer, B., Obara, T., O'Toole, J. F., Hiller, K. S., Mueller, A. M., Ruf, R. G., Hoefele, J., Beekmann, F., Landau, D. et al. (2003). Mutations in INVS encoding inversin cause nephronophthisis type **2**, linking renal cystic disease to the function of primary cilia and left-right axis determination. *Nat. Genet.* **34**, 413-420.

Otto, E. A., Loeys, B., Khanna, H., Hellemans, J., Sudbrak, R., Fan, S., Muerb, U., O'Toole, J. F., Helou, J., Attanasio, M. et al. (2005). Nephrocystin-5, a ciliary IQ domain protein, is mutated in Senior-Loken syndrome and interacts with RPGR and calmodulin. *Nat. Genet.* **37**, 282-288.

Pazour, G. J. (2004). Intraflagellar transport and cilia-dependent renal disease: the ciliary hypothesis of polycystic kidney disease. *J. Am. Soc. Nephrol.* **15**, 2528-2536.

Pazour, G. J., Dickert, B. L., Vucica, Y., Seeley, E. S., Rosenbaum, J. L., Witman, G. B. and Cole, D. G. (2000). Chlamydomonas IFT88 and its mouse homologue, polycystic kidney disease gene Tg737, are required for assembly of cilia and flagella. *J. Cell Biol.* **151**, 709-718.

Perkins, L. A., Hedgecock, E. M., Thomson, J. N. and Culotti, J. G. (1986). Mutant sensory cilia in the nematode Caenorhabditis elegans. *Dev. Biol.* **117**, 456-487.

Praetorius, H. A. and Spring, K. R. (2001). Bending the MDCK cell primary cilium increases intracellular calcium. *J. Membr. Biol.* **184**, 71-79.

Praetorius, H. A. and Spring, K. R. (2003). Removal of the MDCK cell primary cilium abolishes flow sensing. *J. Membr. Biol.* **191**, 69-76.

Qin, H. M., Rosenbaum, J. L. and Barr, M. M. (2001). An autosomal recessive polycystic kidney disease gene homolog is involved in intraflagellar transport in C-elegans ciliated sensory neurons. *Curr. Biol.* **11**, 457-461.

Romio, L., Fry, A. M., Winyard, P. J., Malcolm, S., Woolf, A. S. and Feather, S. A. (2004). OFD1 is a centrosomal/basal body protein expressed during mesenchymal-epithelial transition in human nephrogenesis. *J. Am. Soc. Nephrol.* **15**, 2556-2568.

Sambrook, J., Fritsch, E. F. and Maniatis, T. (1989). *Molecular Cloning: A Laboratory Manual*. New York: Cold Spring Harbor Laboratory Press.

Schafer, J. C., Haycraft, C. J., Thomas, J. H., Yoder, B. K. and Swoboda, P. (2003). XBX-1 encodes a dynein light intermediate chain required for retrograde intraflagellar transport and cilia assembly in Caenorhabditis elegans. *Mol. Biol. Cell* **14**, 2057-2070.

Scholey, J. M. (2003). Intraflagellar transport. *Annu. Rev. Cell Dev. Biol.* **19**, 423-443.

Sengupta, P., Chou, J. H. and Bargmann, C. I. (1996). odr-10 encodes a seven transmembrane domain olfactory receptor required for responses to the odorant diacetyl. *Cell* **84**, 899-909.

Snow, J. J., Ou, G., Gunnarson, A. L., Walker, M. R., Zhou, H. M., Brust-Mascher, I. and Scholey, J. M. (2004). Two anterograde intraflagellar transport motors cooperate to build sensory cilia on C. elegans neurons. *Nat. Cell Biol.* **6**, 1109-1113.

Starich, T. A., Herman, R. K., Kari, C. K., Yeh, W. H., Schackwitz, W. S., Schuyler, M. W., Collet, J., Thomas, J. H. and Riddle, D. L. (1995). Mutations affecting the chemosensory neurons of Caenorhabditis elegans. *Genetics* **139**, 171-188.

Swoboda, P., Adler, H. T. and Thomas, J. H. (2000). The RFX-type transcription factor DAF-19 regulates sensory neuron cilium formation in C. elegans. *Mol. Cell* **5**, 411-421.

Ward, S., Thomson, N., White, J. G. and Brenner, S. (1975). Electron microscopical reconstruction of the anterior sensory anatomy of the nematode Caenorhabditis elegans. *J. Comp. Neurol.* **160**, 313-337.

Ware, R., W., Clark, D., Crossland, K. and Russell, R. L. (1975). The nerve ring of the neamtode Caenorhabditis elegans: sensory input and motor out. *J. Comp. Neurol.* **162**, 71-110.

Wes, P. D. and Bargmann, C. I. (2001). C. elegans odour discrimination requires asymmetric diversity in olfactory neurons. *Nature* **410**, 698-701.

White, J. G., Southgate, E., Thomson, J. N. and Brenner, S. (1986). The structure of the nervous system of the nematode Caenorhabditis elegans. *Philos. Trans. Roy. Soc. London B Biol. Sci.* **314**, 1-340.

Wilson, P. D. (2004). Polycystic kidney disease. *N. Engl. J. Med.* **350**, 151-164.

Wolf, M. T., Lee, J., Panther, F., Otto, E. A., Guan, K. L. and Hildebrandt, F. (2005). Expression and Phenotype Analysis of the Nephrocystin-1 and Nephrocystin-4 Homologs in Caenorhabditis elegans. *J. Am. Soc. Nephrol.* **16**, 676-687.

Zhang, Q., Taulman, P. D. and Yoder, B. K. (2004). Cystic kidney diseases: all roads lead to the cilium. *Physiology* **19**, 225-230.